MATERIALS CHEMISTRY FRONTIERS

CCS 中国化学会 CHINESE CHEMICAL SOCIETY

ICCAS

ROYAL SOCIETY OF CHEMISTRY

Multicolor circularly polarized luminescence: pendant primary amine/diphenylalanine chiral copolymers with clustering-triggered emission

Journal:	*Materials Chemistry Frontiers*
Manuscript ID	QM-RES-03-2024-000228.R1
Article Type:	Research Article
Date Submitted by the Author:	08-Aug-2024
Complete List of Authors:	Yonenuma, Ryo; Yamagata University, Graduate School of Organic Materials Science Takenaka, Aoi ; Yamagata University, Graduate School of Organic Materials Science Nakano, Tamaki; Hokkaido University, Institute for Catalysis Mori, Hideharu; Yamagata University, Graduate School of Organic Materials Science

ARTICLE

Multicolor circularly polarized luminescence: pendant primary amine/diphenylalanine chiral copolymers with clustering-triggered emission

Received 00th January 20xx,
Accepted 00th January 20xx

DOI: 10.1039/x0xx00000x

Ryo Yonenuma,[a] Aoi Takenaka,[a] Tamaki Nakano,[b, c] and Hideharu Mori [a]

Clustering-triggered emission (CTE) materials without π-conjugate chromophores have attracted increasing attention, because of their nonconventional emission properties and wide applications. However, circularly polarized luminescence (CPL) in CTE materials has been less explored. In this study, we designed CTE-based CPL block and random copolymers comprising vinyl amine and *N*-acryloyl-L,L-diphenylalanine. These CTE-based chiral copolymers exhibited concentration- and excited-wavelength-dependent emissions in water. By introducing a charged fluorescent dye (thioflavin T (ThT) or rose bengal) into the copolymer aqueous solution, a red-shifted emission color was detected as the amount of fluorescent dye owing to the fluorescence resonance energy transfer (FRET) between the dye and block copolymers via electrostatic interactions. The chirality of block copolymer was transferred into achiral ThT, as confirmed by ThT-induced circular dichroism. The thin film of CTE-based chiral block copolymer and block copolymer/ThT exhibited CPL, and the chirality of ThT was amplified with the highest emission dissymmetry factor (glum) of -0.9×10^{-3}. This study provides a new perspective on CTE-based CPL polymeric materials, showing CTE-CPL properties in solid states and multicolor CPL by FRET via electrostatic interactions.

Introduction

Luminescent materials have gained wide interest for diverse applications, with the manipulation of emission colors by varying the length of the conjugated electrons in π-conjugated chromophores being a common approach. Such development relies mainly on photochemistry and photophysics.[1-5] However, aggregation-caused quenching (ACQ) poses inherent drawbacks in these materials, hindering their application. Aggregation-induced emission (AIE) has emerged as an alternative system with high emissions in aggregated states.[6-9] Recently, hybrid materials consisting of AIE and chiral molecules, such as amino acids and peptides, have attracted significant attention owing to their unique optoelectronic properties derived from their ability to self-assemble into various nanostructures via noncovalent interactions. Through the rational design of building blocks and linkages, these AIE-chiral molecules occasionally exhibit aggregation-induced circular dichroism (AICD) and circularly polarized luminescence (CPL) derived from achiral AIE molecules via alignment in a chiral environment.[10-19] Particularly, these CPL materials have been explored for applications in three-dimensional display[20-24] and sensing.[25-27]

In our previous study, we developed dipeptide-AIE polymers comprising diphenylalanine and tetraphenylethylene. One is a diphenylalanine-AIE homopolymer from a hybrid monomer with a covalent linkage between diphenylalanine and AIE,[28] and the other is pendant diphenylalanine-AIE copolymers from two diphenylalanine monomers with an AIE comonomer of different compositions.[29] Both of these exhibit the ability to self-assemble into nanostructures (e.g., nanofibers, nanorods, and acicular structures), blue emission, and AICD-derived from tetraphenylethylene units depending on the solvent polarity.

Recently, nonconventional luminescence without π-conjugate chromophores, such as polyethyleneimine,[30] poly(amidoamine),[31-33] poly(*N*-vinyl caprolactam),[34] non-aromatic amino acids[35-38], has emerged as a new class of unique luminescence. These materials contain electron-rich atoms (e.g., N, O, S, P, and Si) and saturated groups (e.g., –OH, $–NH_2$, –COOH, and C–O and C–N bonds). These materials exhibit clustering-triggered emission (CTE) when concentrated or aggregated,[38-41] showcasing potential applications in chemical sensing,[42, 43] bioimaging,[34] and room-temperature phosphorescence.[42-45] However, most CTE materials exhibit blue fluorescence, with limited reports of red-shifted luminescence.[32, 46, 47] While CPL in CTE materials has been less explored, recent efforts have integrated emission dissymmetry factors (g_{lum}) and CTE properties, showing promise for practical applications.[48-51] Compared to conventional CPL materials, CTE-CPL materials offer attractive features such as good processability and water solubility, opening avenues for diverse applications.

[a] *Graduate School of Organic Materials Science, Yamagata University, 4-3-16, Jonan, Yonezawa, 992-8510, Japan, E-mail: h.mori@yz.yamagata-u.ac.jp.*
[b] *Institute for Catalysis (ICAT) and Graduate School of Chemical Sciences and Engineering, Hokkaido University, N21W10, Kita-ku, Sapporo, 001-0021, Japan.*
[c] *Integrated Research Consortium on Chemical Sciences (IRCCS), Institute for Catalysis, Hokkaido University, N21W10, Kita-ku, Sapporo, 001-0021, Japan.*

† Footnotes relating to the title and/or authors should appear here.

Electronic Supplementary Information (ESI) available: [details of any supplementary information available should be included here]. See DOI: 10.1039/x0xx00000x

In this study, we developed new CTE-based CPL block and random copolymers consisting of vinylamine (VAm) with a primary amine as the CTE unit and *N*-acryloyl-L,L-diphenylalanine (APhePheOH) as the chiral dipeptide (L-Phe-L-Phe) unit (Figure 1a). Owing to the ampholytic side-chain structures bearing cationic VAm and anionic APhePheOH units, these CTE-chiral copolymers can be regarded as ampholytic copolymers. By balancing these positive/negative charges, we aimed to achieve amphiphilic properties in neutral water, crucial for self-assembled structures, stimuli responsiveness, and unique CTE-CPL properties. Previously, we synthesized PVAm/amino acid (glutamic acid, lysine)-containing block copolymers with multi-stimuli responsiveness and DNA polyplexes.[52, 53] Furthermore, we reported that VAm-based polyampholytes and cationic copolymers consisting of *N*-acryloyl-L-threonine and its methylated one exhibited characteristic CTE in aqueous solutions with a stimuli-response[54] and polyplex formation.[55] VAm/APhePheOH polyampholytes developed in this study exhibited blue emissions by clusterization at high concentrations in aqueous solution. The emission behavior, self-assembled structures, chiroptical and CTE-CPL properties can be manipulated by internal (e.g., VAm/APhePheOH composition and comonomer sequence; block or random sequence) and external factors (e.g., the concentration, pH of aqueous solutions, and solution/suspension/thin film states). Furthermore, we demonstrate the tuning of the luminescence color by fluorescence resonance energy transfer (FRET) combined with ionic fluorescence dyes and generate induced circular dichroism and CPL derived from achiral fluorescence dyes (Figure 1b). The rational design of chiral ampholytic copolymers, coupled to their self-assemblies and FRET via electrostatic interactions, opens the way towards the development of novel color-tunable CTE-based CPL polymeric materials.

Results and discussion

Synthesis of CTE-based chiral block and random copolymers

CTE-based chiral VAm/APhePheOH block and random copolymers were synthesized via reversible addition–fragmentation chain transfer (RAFT) polymerization of APhePheOH and *N*-vinylphthalimide (NVPI), which was selected as a protected monomer for the preparation of PVAm segment.[52-54, 56, 57] RAFT polymerization of APhePheOH using dithiocarbamate-terminated P(NVPI) macro-chain transfer agent (macro-CTA, $M_{n,NMR}$ = 10700, M_w/M_n = 1.36) at [APhePheOH]/[macro-CTA]/[AIBN] = 50/2/1, 100/2/1, 300/2/1 afforded PNVPI-*b*-PAPhePheOHs with adjustable APhePheOH content between 15% and 37% (Table S1). The NVPI/APhePheOH composition is calculated using ^{1}H NMR spectra to compare the broad peaks at 7.78–6.65 ppm attributed to the aromatic protons of NVPI and APhePheOH and methine protons of APhePheOH at 4.92–4.15 ppm (Figure S1). SEC analysis of methylated PNVPI-*b*-PAPhePheOHs exhibits relatively narrow polydispersities (M_w/M_n = 1.27–1.31) (Figure S3a). The phthalimide moiety from the P(NVPI) segment in the

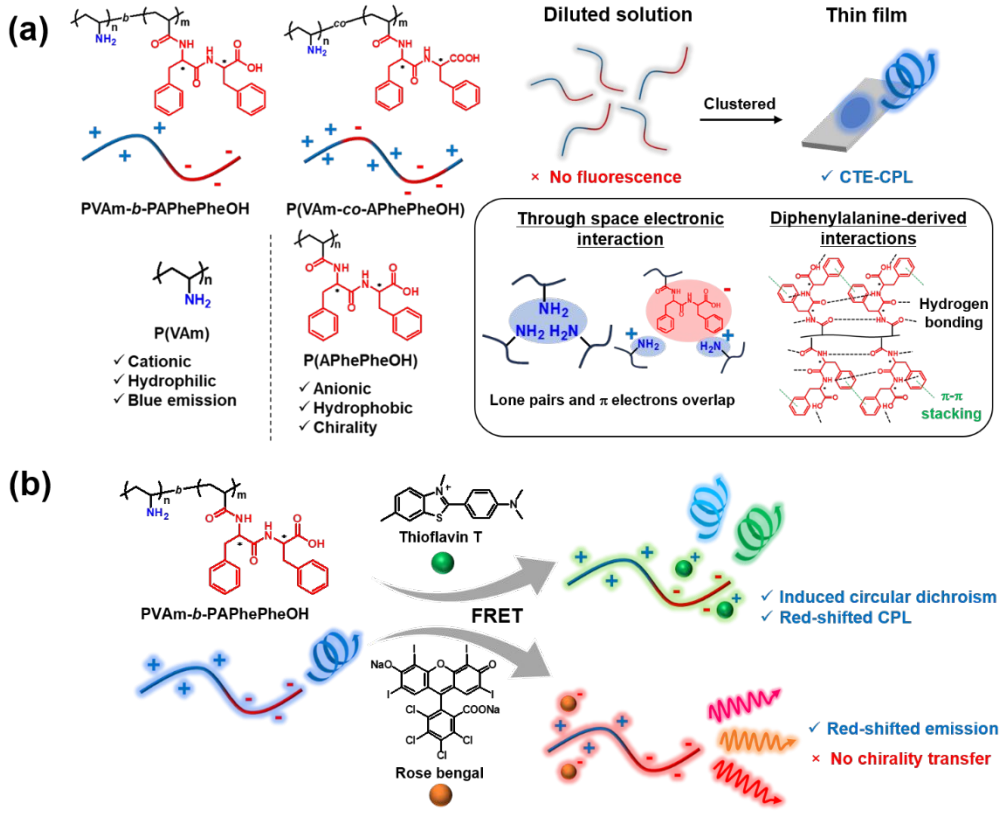

Figure 1. Schematic illustrations of (a) clustering-triggered emission-based chiral block and random copolymers, and (b) multicolor circular polarized luminescence of PVAm-*b*-PAPhePheOH by fluorescence resonance energy transfer with fluorescent dye.

Table 1. Characteristics of CTE-based chiral block and random copolymers consisting of VAm and APhePheOH

Sample	VAm:APhePheOH [a]	Yield [b]	M_n [c] (^{1}H NMR)	M_n [d] (SEC)	M_w/M_n [d] (SEC)
PVAm-*b*-PAPhePheOH	63:37	74	23500	5900	1.31
P(VAm-*co*-APhePheOH)	60:40	80	-	5600	1.37

[a] Prepared by employing RAFT polymerization with AIBN and dithiocarbomate-type CTA followed by hydrazinolysis. [b] Diethyl ether-insoluble fraction. [c] Calculated using ^{1}H NMR spectroscopy of *N*-vinylphtalimide/APhePheOH copolymers in DMSO-d_6. [d] Methylated *N*-vinylphtalimide/APhePheOH copolymers were measured by SEC using PSt standards in DMF (0.01 M LiBr).

block copolymers was removed using hydrazine monohydrate to afford the ampholytic PVAm-*b*-PAPhePheOH. Quantitative deprotection was confirmed by ^{1}H NMR in D_2O to compare the broad peaks at 4.54–3.92 ppm, which can be attributed to the methine protons of APhePheOH and the aromatic protons of APhePheOH at 7.48–6.56 ppm (Figure S1b and Table S3).

Random copolymers P(VAm-*co*-APhePheOH)s were also obtained via RAFT copolymerization and hydrazinolysis. The RAFT copolymerizations of NVPI and APhePheOH with a dithiocarbamate-type RAFT agent at different comonomer feed ratios ([NVPI]/[APhePheOH] = 50/50 and 25/75) were conducted in DMF at 60 °C at $[CTA]_0/[AIBN]_0 = 2$. The resulting random copolymers P(NVPI-*co*-APhePheOH)s were evaluated from the SEC analysis and ^{1}H NMR spectra, showing a predetermined comonomer composition (NVPI:APhePheOH = 78:22 and 60:40) and narrow polydispersity ($M_w/M_n = 1.37$ and 1.41) (Table S2 and Figures S2a and S3b). The hydrazinolysis of the NVPI parts of P(NVPI-*co*-APhePheOH) was conducted using the same procedure as that used for the block copolymer. Target P(VAm-*co*-APhePheOH) was obtained, as confirmed by the ^{1}H NMR results (Figure S2b).

The solubilities of the ampholytic copolymers differed from those of the NVPI-containing precursors. For instance, PNVPI-*b*-PAPhePheOH was soluble in DMSO and DMF. After deprotection, the resulting PVAm-*b*-PAPhePheOH comprising 63% VAm was soluble in neutral and basic water, and insoluble in organic solvents (e.g., DMF and DMSO) and water under acidic conditions (pH < 3) (Table S4). The same tendency was observed in the solubility of the random copolymers: P(VAm-*co*-APhePheOH) comprising 60% VAm was soluble in water (pH = 4, 7, and 12), and the P(NVPI-*co*-APhePheOH) precursor was only soluble in DMF and DMSO (Table S4). PVAm-*b*-PAPhePheOH and P(VAm-*co*-APhePheOH) with similar cation/anion ratios (VAm/APhePheOH = 63/37 and 60/40) and good water solubility (Table 1) were used for further investigation.

Clustering-triggered emission of CTE-based chiral copolymers

UV–Vis and fluorescence measurements of the VAm/APhePheOH block and random copolymers were initially conducted in neutral water (pH 7). The UV–Vis spectrum of PVAm-*b*-PAPhePheOH exhibited absorbance in the range of 250–270 nm, derived from the phenyl rings of the diphenylalanine unit. When the concentration of PVAm-*b*-PAPhePheOH increased, the broad absorption at 300–350 nm corresponding to the n⟶ π * electronic transitions between the amine, amide, and carbonyl groups in the copolymer gradually appeared over 0.5 mg/mL (Figure 2a), which was similar to that observed in other CTE molecules.[42, 54, 58] P(VAm-*co*-APhePheOH) also exhibited absorption at 250–270 nm corresponding to the diphenylalanine group, whereas negligible and weak absorption was detected at 300–350 nm (Figure 2b). The tendency was

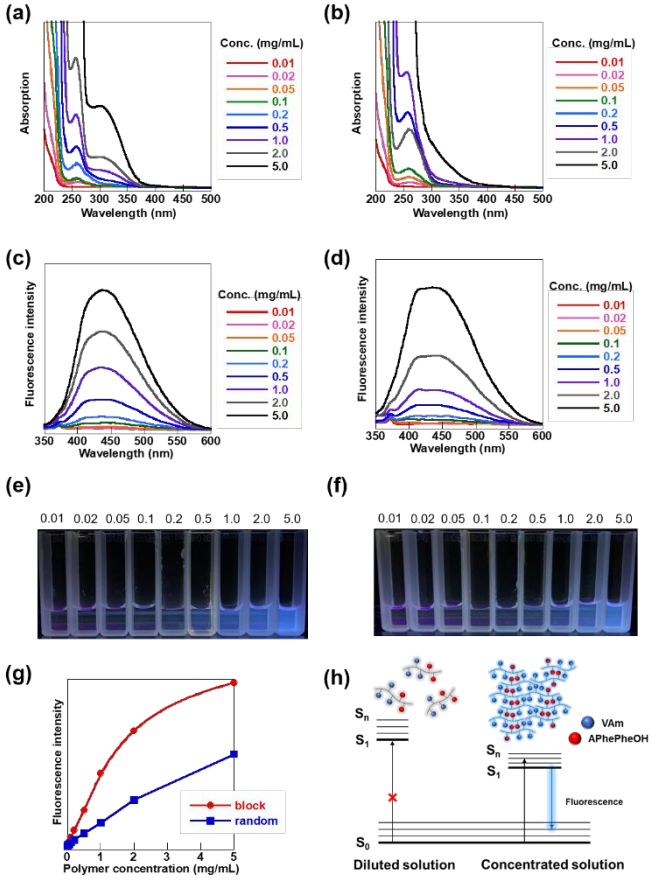

Figure 2. (a, b) UV–Vis spectra at different concentrations, (c, d) concentration-dependent fluorescence spectra (λ_{ex} = 330 nm), and (e, f) their photograph captured under 365 nm UV light of (a, c, e) PVAm-*b*-PAPhePheOH and (b, d, f) P(VAm-*co*-APhePheOH) in water (pH = 7). (g) Fluorescence intensity of PVAm-*b*-PAPhePheOH and P(VAm-*co*-APhePheOH) (λ_{ex} = 330 nm) against polymer concentration in water (pH = 7, conc. = 0.01–5.0 mg/mL). (h) Proposed Jablonski diagrams of PVAm-*b*-PAPhePheOH in diluted and concentrated solutions.

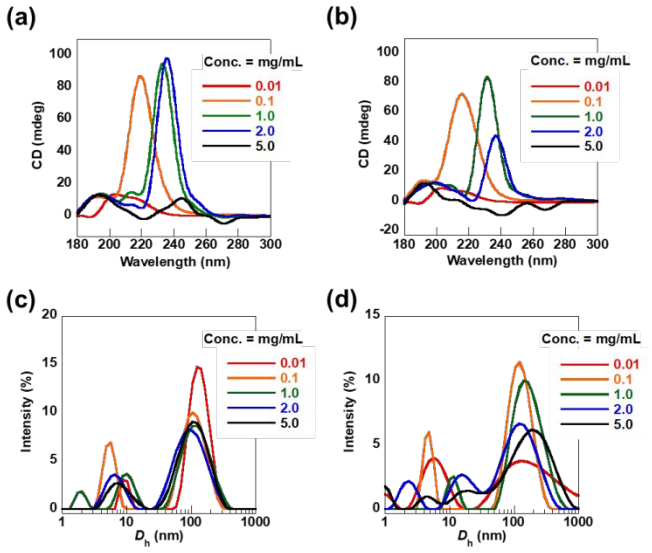

Figure 3. (a, b) Circular dichroism (CD) spectra and (c, d) DLS traces of (a, c) PVAm-*b*-PAPhePheOH and (b, d) P(VAm-*co*-APhePheOH) in water (pH = 7).

distinct from the PVAm homopolymer, which exhibited broad absorption at 300–350 nm derived from the n→ π * transition by clustering of the VAm unit in the homopolymer side chain with increasing polymer concentration (Figure S4a). These results indicate that the comonomer sequence affects the states of the n→ π * transition at different concentrations of the assembled structures.

The fluorescence spectrum of PVAm-*b*-PAPhePheOH exhibited a broad peak at 437 nm (λ_{ex} = 330 nm), and the emission intensity increased with increasing concentration (Figure 2c). A similar emission behavior was observed for P(VAm-*co*-APhePheOH) as its concentration increased from 0.01 to 5.0 mg/mL and the maximum emission wavelength was 435 nm (Figure 2d). These results indicate a common feature found in various CTE polymers, exhibiting clusteroluminescence in condensed states (high concentrations) and nonluminescence in diluted states (low concentrations).[38-41] When irradiated with UV light, blue emission enhancement was detected visually with an increase in the concentration of block and random copolymers (Figures 2e, 2f). As shown in Figure 2g, the block copolymer exhibited a higher concentration-induced emission enhancement than the random copolymer. Blue luminescence at high polymer concentrations was observed for the PVAm homopolymer (Figure S4), exhibiting red-shifted emission with a maximum wavelength of 471 nm in water (pH = 7). The quantum yields of the PVAm, PVAm-*b*-PAPhePheOH and P(VAm-*co*-APhePheOH) were 1.4 %, 6.3 %, 4.8 %, respectively (Table S5). Similar to other CTE systems via through-space interactions,[38-41] the clustering of the primary amino group in VAm unit induced by APhePheOH-based interactions leads to an increase in the excitation energy to reach an excited state (S_n) at a high concentration, and the consumption of excitation energy results in the characteristic fluorescence (Figure 2h). Probably, production of emissive J-aggregation along with transition dipole-dipole interaction is an important factor. Nevertheless, the emissions by clusterization at high concentrations is predominant over the J-aggregation in the present system.

A characteristic of CTE materials is that they exhibit different emission wavelengths depending on the excitation wavelength.[54, 58] Therefore, we investigated the excitation wavelength-dependent emission of the CTE-chiral block and random copolymers. When irradiated with different excitation wavelengths, PVAm-*b*-PAPhePheOH exhibited the strongest emission peaks at 285 and 290 nm (λ_{ex} = 254 and 270 nm) derived from phenylalanine moieties, and peaks at 420–438 nm (λ_{ex} = 290–400 nm) (Figure S5a) derived from VAm-based clusters and APhePheOH-based clusters. The maximum fluorescence intensity of PVAm-*b*-PAPhePheOH was observed at 437 nm (λ_{ex} = 330 nm), whereas the fluorescence intensity decreased significantly when the excitation wavelength was increased to 380 and 400 nm. P(VAm-*co*-APhePheOH) also exhibited similar emission behavior (Figure S5b), even though the wavelength-dependent change in fluorescence was less than that of the block copolymer. These results indicate that the copolymer sequence affects wavelength-dependent emission behavior. Probably, the production of several aggregated structures originating from intermolecular and intramolecular side-chain interactions, and J- and H-aggregation, are responsive for the excitation wavelength dependency, which are affected by the copolymer sequence.

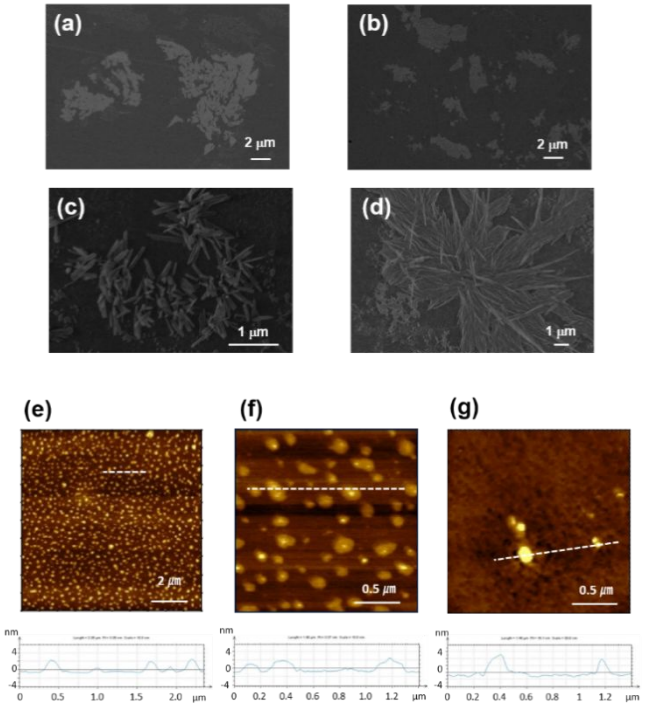

Figure 4. (a-d) Scanning electron microscopy (SEM) and (e-g) atomic force microscopy (AFM) height images of (a, c, e, f) PVAm-*b*-PAPhePheOH and (b, d, g) P(VAm-*co*-APhePheOH). The samples were prepared from aqueous solutions (conc. = 2.0 mg/mL) at different pHs, (a-b, e-g) pH 7, (c-d) pH 12. (e-g) Cross sections through the lines indicated by the dotted line in the AFM height images.

CD, DLS, and zeta potential measurements of the VAm/APhePheOH block and random copolymers were conducted to elucidate the relationship between the assembled structures and the chiroptical and CTE properties. The CD

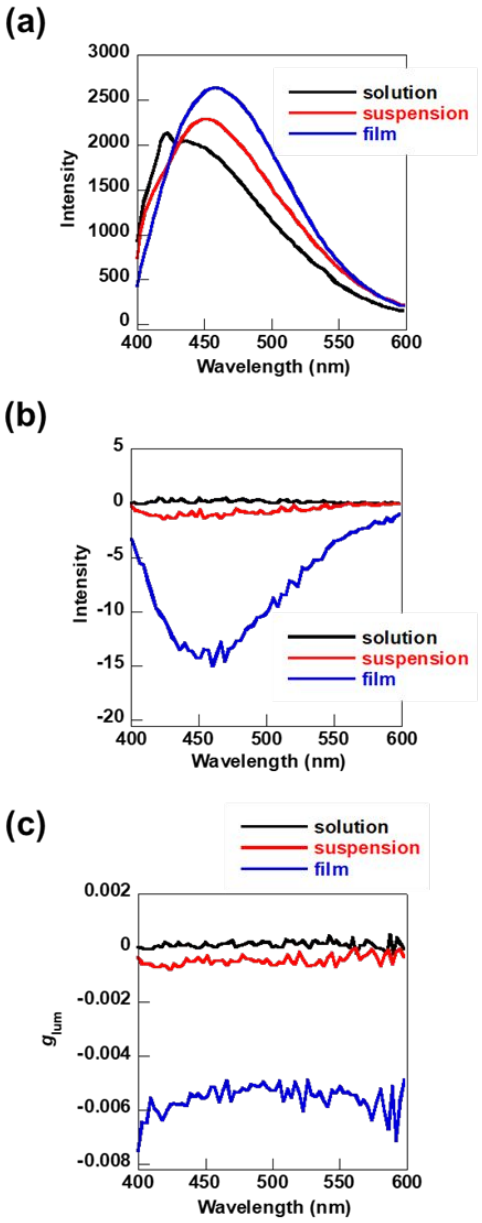

Figure 5. (a) Emission spectra, (b) circularly polarized luminescence (CPL) spectra, and (c) g_{lum} spectra of PVAm-*b*-PAPhePheOH in different states (solution: water (pH = 7, conc. = 2.0 mg/mL); suspension: water/THF = 4/96 (conc. = 2.0 mg/mL); thin film prepared from PVAm-*b*-PAPhePheOH aqueous solutions (pH = 7, conc. = 20.0 mg/mL), λ_{ex} = 350 nm).

spectra show that PVAm-*b*-PAPhePheOH in water (pH = 7, conc. = 1.0 and 2.0 mg/mL) exhibited a positive peak at approximately 235 nm, which was derived from the phenyl rings of the diphenylalanine moieties (Figure 3a). The strong peak of the aromatic rings at 220 nm exhibited a blue-shift at lower concentrations (conc. = 0.1 mg/mL) and was undetectable at even lower concentrations (0.01 mg/mL), indicating that the formation of different aggregated structures is influenced by specific interactions, such as hydrogen bond, hydrophobic interaction, and π–π stacking, between the diphenylalanine moieties, which are dependent on the concentrations and on β-sheet content.[59] P(VAm-*co*-APhePheOH) showed similar behavior, but when the concentration of the random copolymer was over 1.0 mg/mL, the diphenylalanine-derived peak decreased gradually (Figures 3b and S6). In both cases, the positive CD peak was hardly detected at a higher concentration (5.0 mg/mL), implying that the VAm units inhibit β-sheet structure formation in a highly condensed state by interfering with the diphenylalanine-derived interactions. The origin of redshift in CD and CD spectral inversion with increasing the concentration from 0.01 into 5.0 mg/mL, as shown in Figures 3a and 3b, is substantial conformational transitions, owing to the concentration-depending aggregations.

The intensity-average hydrodynamic diameter (D_h) of PVAm-*b*-PAPhePheOH was initially determined in an aqueous solution at pH 7 using DLS measurements (Figures 3c and 3d). The PVAm-*b*-PAPhePheOH solution exhibited constant size (D_h = 109–138 nm) in the concentration range of 0.1–5.0 mg/mL in the presence of small species (< 10 nm) at every concentration, which can be attributed to unimolecular and/or smaller aggregated states (Figure 3c). P(VAm-*co*-APhePheOH) exhibited multimodal peaks at all concentrations, indicating the presence of various assemblies/aggregates in an aqueous solution (Figures 3d and S7). The zeta potentials of PVAm-*b*-PAPhePheOH and P(VAm-*co*-APhePheOH) exhibited a slightly positive charge in neutral water (pH = 7) (Figures S8c, S8d, Table S6), revealing that the copolymers self-assembled into micelle-like structures with PVAm shells and PAPhePheOH cores originating from the compositions (60%–63% VAm contents). From these results, it can be inferred that various sizes of assemblies/aggregates exist in an aqueous solution, and heterogeneous clusters are formed by amine, amide, and carbonyl groups, generating different sizes of spatial electron delocalization.[58] Therefore, the CTE-based chiral block and random copolymers may exhibit excitation wavelength-dependent emission. The remarkable concentration effects observed in this work may at least partially be connected to Mie scattering.[60-64] It is known that CD spectra and optical rotatory dispersion (ORD) of poly(L-glutamic acid) are affected by the presence of aggregates whose radius is as small as 0.03 micrometers. In addition, Mie effects on CPLm systems have also been reported.[65] Because the polymers discussed here have a D_h of 100 nm or greater, Mie scattering as well as changes in polymer conformation and chiral aggregates depending on concentration can affect the chiroptical properties.

Scanning electron microscopy (SEM) measurements were conducted to investigate the self-assembly behavior of the CTE-based chiral block and random copolymers (Figure 4). When the samples were prepared from a neutral aqueous solution (pH 7, conc. = 2.0 mg/mL), aggregate formation of PVAm-*b*-PAPhePheOH and P(VAm-*co*-APhePheOH) occurred (Figures 4a and 4b). Atomic force microscopy (AFM) heigh image of the block copolymer sample prepared from the aqueous solution (2.0 mg/L, pH 7) showed homogeneous spherical structures with 100–200 nm in diameter and 2–4 nm in height (Figures 4e and 4f), possibly corresponding to the collapsed micelles formed on the mica substrate. The same morphology was observed in the AFM phase images (Figure S9), implying the referable formation of stable micelles in neutral water. In

contrast, the random copolymer sample prepared under the same condition occasionally showed assembled structures (Figures 4g and S10). These results indicate that the copolymer sequence has a substantial effect on chiroptical properties and assembled structures.

Effect of pH on CTE property and assembled structures

APhePheOH and PAPhePheOH exhibited a deep blue luminescence with maximum emission wavelengths of 431 and 411 nm when dissolved in a basic aqueous solution (pH 12, conc. of 2.0 mg/mL) (Figure S11). Note that PAPhePheOH was only soluble in water under basic conditions (pH = 12) and insoluble at pH 7.[66] These results suggested that PAPhePheOH also forms clusters owing to β-sheet-like structures formed by hydrogen bonds between the amide and carbonyl groups. Therefore, the CTE-chiral block and random copolymers demonstrated two clusters derived from the VAm and APhePheOH units, respectively, and their sequence (block and random) affected the maximum emission peak position and concentration-dependent emission behavior. Ampholytic block and random copolymers might show different emission behaviors owing to the protonated or deprotonated states of the amino groups and carboxy groups after changing the pH of the aqueous solution.[67] Although the emission intensity was slightly affected by pH values, the VAm/APhePheOH block and random copolymers exhibited similar emission behavior (Figures S12 and S13).

DLS traces of PVAm-*b*-PAPhePheOH exhibited bimodal peaks corresponding to unimolecular and assembled states at different pH values (pH = 4–12), indicating the formation of self-assembled structures that are independent of pH (Figure S8a and Table S6). In contrast, P(VAm-*co*-APhePheOH) exhibited multimodal peaks at all pH values, implying the presence of aggregates of various sizes in the solution (Figure S8b). SEM images showed characteristic assembled structures formed under basic conditions (pH 12, Figures 4c and 4d), which were apparently distinct from the samples prepared in neutral water (pH 7, Figures 4a and 4b). Both the block and random copolymers self-assembled into microcrystals and formed fractal patterns, probably owing to the attraction force between Na^+ ions and the COO^- groups of APhePheOH during the drying of the solutions on the substrate, as observed in carboxylate-containing amino acid derivatives and polymeric materials.[68-70]

CTE-based CPL of PVAm-*b*-PAPhePheOH at different states

The CPL measurements of PVAm-*b*-PAPhePheOH were conducted in different states (e.g., solutions, suspensions, and thin films). In the solution state, neutral water was selected as a good solvent (conc. = 2.0 mg/mL, pH = 7), a water/THF mixture with THF as the poor solvent was used as the selective solvent (water/THF = 4/96, conc. = 2.0 mg/mL) and added to the suspension. Here, the block copolymer was selected for CPL measurements, owing to higher CD signals and preferable formation of assembled structures, compared to the random copolymer. Thin films were prepared by drop-casting highly concentrated PVAm-*b*-PAPhePheOH aqueous solutions (conc. = 20.0 mg/mL, pH = 7) and dried at 100 °C until the solvent had dried in the atmosphere. As shown in Figure 5a, the maximum emission wavelength exhibited a red-shift as the state changed from solution (422 nm) to suspension (451 nm) and thin film (457 nm), suggesting that more condensed clusters are formed in the thin film state. Furthermore, the PVAm-*b*-PAPhePheOH thin film exhibited a strong right-handed CPL (Figure 5b). The emission dissymmetry factor (g_{lum}) was −0.0051 and more than 10 times higher than that of the solution and suspension states (Figure 5c and Table S7). These spectra were measured at two angles of the PVAm-*b*-PAPhePheOH thin film, vertically and horizontally (Figure S14). Although the CPL intensity changed slightly depending on the angle, the shapes and signs of the CPL spectra were largely identical, indicating that the resulting CPL was based on the chirality of the APhePheOH units.

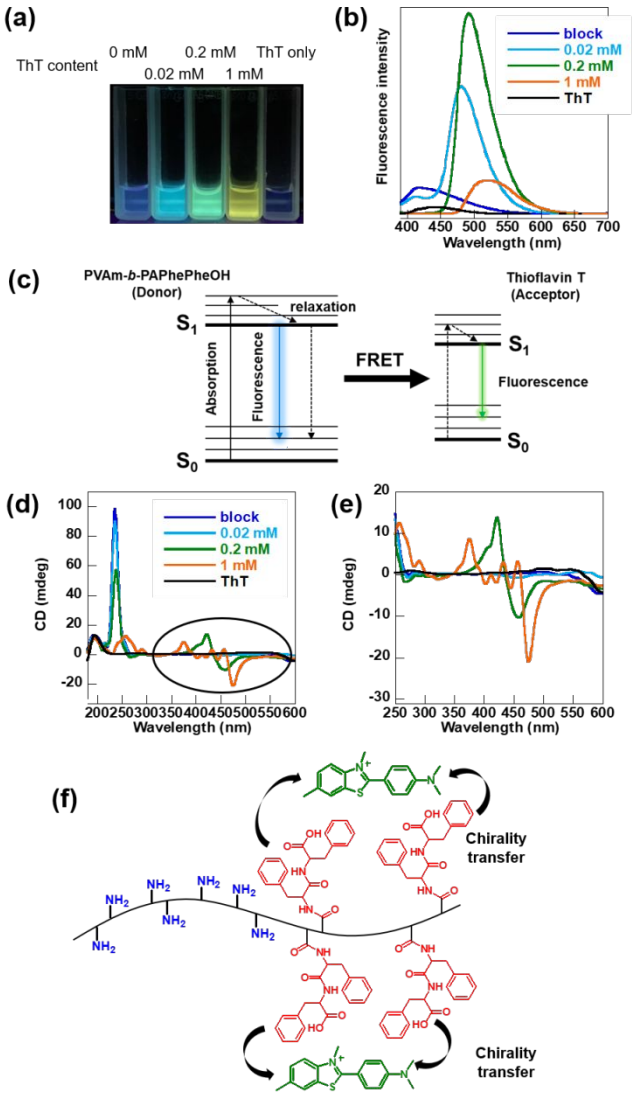

Figure 6. (a) Photograph of PVAm-*b*-PAPhePheOH and different molar ratio of thioflavin T (ThT) in water captured under 365 nm UV light (polymer conc. = 2.0 mg/mL, ThT = 0–1 mM), (b) fluorescence spectra (λ_{ex} = 365 nm), and (c) proposed Jablonski diagram of a FRET process following light absorption by PVAm-*b*-PAPhePheOH donor. (d, e) CD spectra of PVAm-*b*-PAPhePheOH and different molar ratios of ThT in water. (f) Schematic illustration of chirality transfer from PVAm-*b*-PAPhePheOH to ThT.

Fluorescence resonance transfer energy with ionic fluorescence dye

PVAm-*b*-PAPhePheOH can undergo FRET, similar to its conjugated counterpart, to adjust its color. Recently, Yan et al. reported that color-tunable CPL generated with polylysine/oleate ion CTE was obtained via FRET using appropriate acceptor (fluorescein solidum).[48] In this study, we selected thioflavin T (ThT) and rose bengal (RB) as the cationic and anionic commercial fluorescent dyes, respectively (Figures 6 and 7). ThT is frequently used for amyloid fibril detection,[71, 72] as it absorbs light at 380–450 nm and emits strong green fluorescence near 490 nm via restricted rotation. RB also absorbs at 450–580 nm and emits near 590 nm.[73, 74] Because the emission of PVAm-*b*-PAPhePheOH in neutral water overlaps well with the absorption of ThT or RB, the fluorescent dye is doped as an energy acceptor into the solution via electrostatic interactions (Figure S15). Figure 6 shows FRET between PVAm-*b*-PAPhePheOH and ThT. With an increase in the amount of fluorescent dye, the blue emission of PVAm-*b*-PAPhePheOH decreases gradually, and the emission color changes to light blue, green, or yellow with the addition of ThT (Figures 6a and 6b). In FRET process, PVAm-*b*-PAPhePheOH (donor) absorbs incident light and transfer the energy to ThT (acceptor), as shown in Figure 6c. Maximum fluorescent dye emission was observed at a ThT doping rate of 0.2 mM. The quantum yield of PVAm-*b*-PAPhePheOH/ThT was 25.6 % (Table S8), which was lower than that of ThT interacted with amiloyd fibrils (43-44 %).[75, 76] The increase in the quantum yield upon co-aggregation with ThT is probably due to efficient absorption of the blue emission from block copolymer, and restriction of free rotation of the benzothiazole unit by the specific interaction between ThT and the copolymer. So-called deactivation of vibrational, rotational, and librational modes in the dyes and the copolymers in their homogeneous solutions are also important factor. The FRET efficiency[77] determined from the quenching of the copolymer donor fluorescence intensity in the absence and presence of ThT as the acceptor molecule (Eq. S2) was 0.98 (Table S8). Further increase in the fluorescent dye resulted in a decrease of the emission intensity and quantum yield (5.8 %, Table S8), attributed to the formation of excimers or ACQ (Figure S16).[78]

Furthermore, the chirality of PVAm-*b*-PAPhePheOH was also transferred to ThT, resulting in a positive CD signal at 422 nm and a negative signal at 459 nm and 0.2 mM of ThT (Figures 6d-f), indicating that ThT is located near the anionic diphenylalanine moieties owing to the electrostatic interaction in solution. The absorption dissymmetry factor (g_{abs}) was 1.66 $\times$ 10^{-4} at 422 nm with a ThT doping ratio of 0.2 mM (Table S9). DLS measurements showed that the size of the complexes formed between PVAm-*b*-PAPhePheOH and ThT increased with an increase in the doping ratio of ThT (Figure S17a) until the doping ratio reached 0.2 mM. The size of the complex then decreased (e.g., D_h = 122 and 32 nm at 0.2 and 1 mM of ThT). The zeta potential of the PVAm-*b*-PAPhePheOH/ThT complex at 0.2 mM was almost zero, which changed to positive (approximately 10 mv at 0.02 mM) and negative (approximately −20 mv at 1.0 mM of ThT) values, depending on the doping rate (Figure S17b, Table S10). For comparison, the emission behaviors of the PVAm homopolymer complex and P(VAm-*co*-APhePheOH) with ThT were evaluated under the same conditions. The PVAm homopolymer exhibited blue emission derived from the CTE of PVAm, without any change in the emission wavelength, indicating no energy transfer between PVAm and ThT (Figures S18 and S19a). P(VAm-*co*-APhePheOH) exhibited red-shifted emission when combined with ThT (Figure S19b), which was similar to that of PVAm-*b*-PAPhePheOH. The fluorescence energy from P(VAm-*co*-APhePheOH) to ThT was less efficient, which may be attributed to limited electrostatic interactions between ThT and APhePheOH units randomly distributed in P(VAm-*co*-APhePheOH). The comonomer sequence exhibited a substantial effect on the induced CD derived from the APhePheOH unit in ThT. The P(VAm-*co*-APhePheOH)/ThT complex solution exhibited weaker CD spectra and lower g_{abs} (5.04×10^{-4}) than PVAm-*b*-PAPhePheOH complex (Figure S20, Table S11). Tunable color and induced circular dichroism, derived from the VAm/APhePheOH copolymers incorporated ThT obtained by adding a fluorescent dye to the APhePheOH acceptors, were achieved through the FRET process.

Figure 7 shows FRET between PVAm-*b*-PAPhePheOH and RB. The blue emission of PVAm-*b*-PAPhePheOH gradually decreased with an increase in the amount of RB, and consequently, red-shifted emissions, such as pink, orange, and red, derived from RB were observed (Figures 7a and 7b). The maximum fluorescence dye emission intensity (592 nm) was observed at an RB doping rate of 0.2 mM and a further increase in the fluorescence dye resulted in decreased emission intensity (Figure S21). The quantum yields also increased as the amount of RB (Table S12). Similar to the block copolymer/ThT, the FRET efficiency increased from 0.35 into 0.99 with increasing the RB doping rate from 0.02 into 1.0 mM. Furthermore, a block

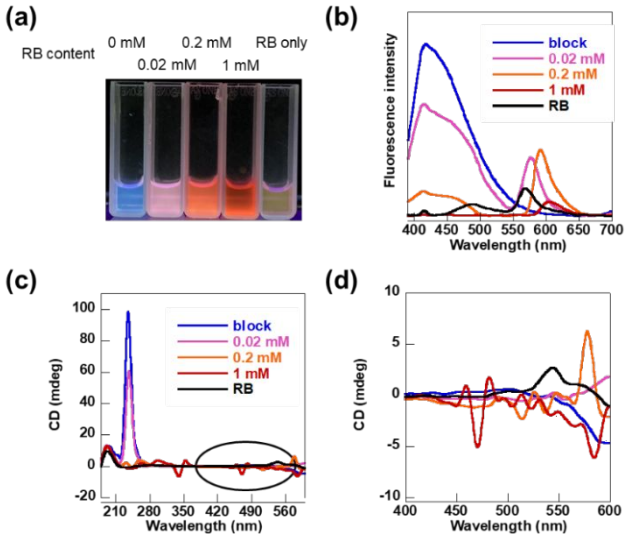

Figure 7. (a) Photograph of PVAm-*b*-PAPhePheOH and different molar ratios of RB in water captured under 365 nm UV light (polymer conc. = 2.0 mg/mL, RB = 0–1 mM), (b) fluorescence spectra (λ_{ex} = 365 nm), and (c, d) CD spectra of PVAm-*b*-PAPhePheOH and different molar ratios of RB in water.

copolymer/RB complex exhibited a slightly longer red-shifted emission (λ_{em} = 592 nm) than the VAm/APhePheOH random copolymer/RB complex (λ_{em} = 584 nm), indicating that the comonomer sequence affects the emission behavior (Figure S22). The quantum yields were also No remarkable CD peak transfer from PVAm-*b*-PAPhePheOH to RB was observed (Figures 7c and 7d), signifying substantial contribution of anionic RB to the electrostatic repulsion between RB and anionic diphenylalanine moieties (Figure S23).

Red-shifted CPL by PVAm-*b*-PAPhePheOH and ThT

CPL measurements of PVAm-*b*-PAPhePheOH/ThT complexes were performed (Figure 8). Initially, the PVAm-*b*-PAPhePheOH/ThT complexes prepared in different states (solution and thin films, Figure S24) were compared. The emission of the PVAm-*b*-PAPhePheOH/ThT complexes exhibited a red-shift in the thin-film state compared with that in the aqueous solution state, suggesting that the CTE-based chiral block copolymer and ThT are more aggregated in the thin-film state (Figure 8a). The CPL spectra also showed right-handed CPL in both solution and thin-film states. The CPL intensity and emission dissymmetry factor (g_{lum}) were higher in the thin-film state than in the solution state (Figures 8b and 8c). The g_{lum} of the thin film state was −0.00577, which was more than 600 times that of the solution state (Table S13).

Next, we measured the CPL spectra of thin films prepared from PVAm-*b*-PAPhePheOH with different ThT molar ratios (Figures 8d and S25-S27). The fluorescence spectra exhibited red-shift emission (Figure 8d) with increasing ThT concentration, similar to the emission behavior observed in solution (Figure 8b), and all thin films exhibited right-handed CPL (Figure 8e). The highest emission dissymmetry factor (g_{lum}) was −0.0099 at 486 nm, with a ThT doping rate of 0.02 mM (Figure 8f, Table S14). Tunable CPL can be achieved through FRET by tuning the amount and amplifying the chirality of the achiral fluorescent dye. The negative CPL from dyes is probably due to the induced axial chirality between benzothiaziazole and phenyl units in ThT. Similar tendency was reported in CD and CPL spectra of ThT bound to amyloid fibrils, showing Cotton effects induced by an aromatic ring close to the ThT via stabilization of one enantiomeric conformer.[79] As control experiments, we prepared samples using two different procedures at pH 7, firstly preparing the copolymer solution, followed by adding dye, and firstly preparing the dye solution, followed by adding copolymer. Substantial difference was detected in DLS, Zeta potential, and CD results (Figures S28-S30 and Table S15-S16). The highest Cotton effect was observed in the copolymer/ThT sample, firstly preparing the ThT solution, followed by adding copolymer. In this procedure, chiral copolymer may be attached or surrounded to its opposite charged surface of the dye homo-aggregates. Hence, the sample preparation procedure is also a crucial factor to achieve characteristic CD/CPL properties. Various factors, such as the donor-acceptor distance, spatial arrangement and orientational behavior, the donor quantum yield, and the refractive index of the medium, are crucial to optimize FRET process.[77] Further studies, such as PL excitation and CP excitation spectral measurements, investigation of PL dynamics, and Förster distance calculations, will help to understand detailed mechanisms and achieve improved CTE-CPL properties.

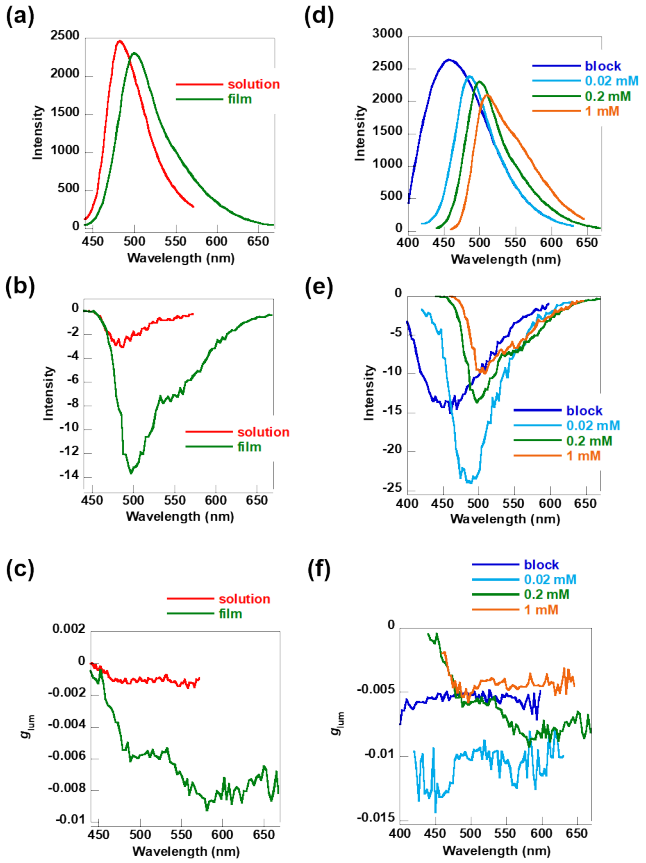

Figure 8. (a, d) Emission spectra, (b, e) CPL spectra, and (c, f) g_{lum} spectra, (a, b, c) comparison of solution state and thin film state of PVAm-*b*-PAPhePheOH/ThT complex (polymer conc. = 10.0 mg/mL, ThT conc. = 0.2 mM, λ_{ex} = 350 nm), and (d, e, f) thin films of PVAm-*b*-PAPhePheOH with different ThT molar ratios.

Conclusion

The CTE-based chiral VAm/APhePheOH block and random copolymers exhibiting CTE-based CPL were synthesized via RAFT polymerization and subsequent hydrazinolysis. The emission intensity was substantially affected by the concentration, wavelength, and comonomer sequence (block vs. random). The characteristic CTE behavior has been attributed to various non-covalent interactions, including hydrogen bonds, electrostatic interactions, and π–π stacking between the primary amines originating from VAm, carboxylic acid and amide moieties, and the aromatic rings from APhePheOH. The PVAm-*b*-PAPhePheOH block copolymer could interact with the ionized fluorescent dye via electrostatic interactions, yielding complexes that exhibited red-shift luminescence (with ThT: light blue to green, yellow; with RB: pink to orange, red). When ThT interacted with PVAm-*b*-PAPhePheOH, ThT exhibited induced circular dichroism in the CD spectra. Thin films of PVAm-*b*-PAPhePheOH/ThT complexes exhibited right-handed

CPL with emission dissymmetry factors between -0.004 and close to -0.01 by tuning the ratio of ThT. This finding substantially broadens the versatility of CTE-based CPL polymeric materials, combining the chiral self-assembling unit and nonconjugated CTE unit. This study also represents a novel approach to achieving CPL using CTE-based chiral copolymers. These CTE-chiral polymers and CTE-chiral polymer/fluorescent dye complexes exhibiting CPL show promise for future bio-related and optoelectronic applications such as bioimaging, sensing.

Conflicts of interest

There are no conflicts to declare.

Acknowledgements

This work was supported by the JST and the establishment of university fellowships for the creation of science and technology innovation (Grant Number JPMJFS2104).

Notes and references

1 J. R. Lakowicz, *Principles of fluorescence spectroscopy, 3rd Edition*, Springer, 2007.

2 N. J. Turro, V. Ramamurthy and J. C. Scaiano, *Modern molecular photochemistry of organic molecules*, University Science Books, 2010.

3 M. Kasha, H. R. Rawls and M. A. El-Bayoumi, The exciton model in molecular spectroscopy, *Pure and Applied Chemistry*, 1965, **11**, 371-392.

4 T. J. Dougherty, Photosensitizers - therapy and detection of malignat tumors *Photochemistry and photobiology*, 1987, **45**, 879-889.

5 V. Ramamurthy and N. Turro, Photochemistry-Introduction *Chemical Reviews*, 1993, **93**, 1-2.

6 J. Luo, Z. Xie, J. Lam, L. Cheng, H. Chen, C. Qiu, H. Kwok, X. Zhan, Y. Liu, D. Zhu and B. Tang, Aggregation-induced emission of 1-methyl-1,2,3,4,5-pentaphenylsilole, *Chemical Communications*, 2001, **18**, 1740-1741.

7 Y. Hong, J. W. Y. Lam and B. Z. Tang, Aggregation-induced emission, *Chem. Soc. Rev.*, 2011, **40**, 5361-5388.

8 X. Cai and B. Liu, Aggregation-Induced Emission: Recent Advances in Materials and Biomedical Applications, *Angew. Chem. Int. Ed.*, 2020, **59**, 9868-9886.

9 R. Hu, A. Qin and B. Z. Tang, AIE polymers: Synthesis and applications, *Prog. Polym. Sci.*, 2020, **100**, 101176.

10 H. Li, J. Cheng, Y. Zhao, J. W. Y. Lam, K. S. Wong, H. Wu, B. S. Li and B. Z. Tang, l-Valine methyl ester-containing tetraphenylethene: aggregation-induced emission, aggregation-induced circular dichroism, circularly polarized luminescence, and helical self-assembly, *Mater. Horiz.*, 2014, **1**, 518-521.

11 H. Li, X. Zheng, H. Su, J. W. Y. Lam, K. S. Wong, S. Xue, X. Huang, X. Huang, B. S. Li and B. Z. Tang, Synthesis, optical properties and helical self-assembly of a bivaline-containing tetraphenylethene, *Sci. Rep.*, 2016, **6**, 19277.

12 B. S. Li, R. Wen, S. Xue, L. Shi, Z. Tang, Z. Wang and B. Z. Tang, Fabrication of circular polarized luminescent helical fibers from chiral phenanthro[9,10]imidazole derivatives, *Mater. Chem. Front.*, 2017, **1**, 646-653.

13 G. Huang, R. Wen, Z. Wang, B. S. Li and B. Z. Tang, Novel chiral aggregation induced emission molecules: self-assembly, circularly polarized luminescence and copper(ii) ion detection, *Mater. Chem. Front.*, 2018, **2**, 1884-1892.

14 S. P. Goskulwad, M. A. Kobaisi, D. D. La, R. S. Bhosale, M. Ratanlal, S. V. Bhosale and S. V. Bhosale, Supramolecular Chiral Helical Ribbons of Tetraphenylethylene-Appended Naphthalenediimide Controlled by Solvent and Induced by l- and d-Alanine Spacers, *Chem. Asian J.*, 2018, **13**, 3947-3953.

15 Q. Liu, Q. Xia, S. Wang, B. S. Li and B. Z. Tang, In situ visualizable self-assembly, aggregation-induced emission and circularly polarized luminescence of tetraphenylethene and alanine-based chiral polytriazole, *J. Mater. Chem. C*, 2018, **6**, 4807-4816.

16 S. P. Goskulwad, V. G. More, M. A. Kobaisi, R. S. Bhosale, D. D. La, F. Antolasic, S. V. Bhosale and S. V. Bhosale, Solvent ‐ Induced Self ‐ Assembly of Naphthalenediimide Conjugated to Tetraphenylethene through D ‐ and L ‐ Alanine, *ChemistrySelect*, 2019, **4**, 2626-2633.

17 Y. Shi, G. Yin, Z. Yan, P. Sang, M. Wang, R. Brzozowski, P. Eswara, L. Wojtas, Y. Zheng, X. Li and J. Cai, Helical Sulfono-γ-AApeptides with Aggregation-Induced Emission and Circularly Polarized Luminescence, *J. Am. Chem. Soc.*, 2019, **141**, 12697-12706.

18 Q. Liu, Q. Xia, Y. Xiong, B. S. Li and B. Z. Tang, Circularly Polarized Luminescence and Tunable Helical Assemblies of Aggregation-Induced Emission Amphiphilic Polytriazole Carrying Chiral l-Phenylalanine Pendants, *Macromolecules*, 2020, **53**, 6288-6298.

19 Y. Wang, D. Niu, G. Ouyang and M. Liu, Double helical pi-aggregate nanoarchitectonics for amplified circularly polarized luminescence, *Nat. Commun.*, 2022, **13**, 1710.

20 D.-M. Lee, J.-W. Song, Y.-J. Lee, C.-J. Yu and J.-H. Kim, Control of Circularly Polarized Electroluminescence in Induced Twist Structure of Conjugate Polymer, *Adv. Mater.*, 2017, **29**, 1700907.

21 F. Zinna, M. Pasini, F. Galeotti, C. Botta, L. Di Bari and U. Giovanella, Design of Lanthanide-Based OLEDs with Remarkable Circularly Polarized Electroluminescence, *Adv. Funct. Mater.*, 2017, **27**, 1603719.

22 J. Han, S. Guo, J. Wang, L. Wei, Y. Zhuang, S. Liu, Q. Zhao, X. Zhang and W. Huang, Circularly Polarized Phosphorescent Electroluminescence from Chiral Cationic Iridium(III) Isocyanide Complexes, *Adv. Opt. Mater.*, 2017, **5**, 1700359.

23 F. Song, Z. Xu, Q. Zhang, Z. Zhao, H. Zhang, W. Zhao, Z. Qiu, C. Qi, H. Zhang, H. H. Y. Sung, I. D. Williams, J. W. Y. Lam, Z. Zhao, A. Qin, D. Ma and B. Z. Tang, Highly Efficient Circularly Polarized Electroluminescence from Aggregation-Induced Emission Luminogens with Amplified Chirality and Delayed Fluorescence, *Adv. Funct. Mater.*, 2018, **28**, 1800051.

24 M. Li, S.-H. Li, D. Zhang, M. Cai, L. Duan, M.-K. Fung and C.-F. Chen, Stable Enantiomers Displaying Thermally Activated Delayed Fluorescence: Efficient OLEDs with Circularly Polarized Electroluminescence, *Angew. Chem. Int. Ed.*, 2018, **57**, 2889-2893.

25 S. P. Morcillo, D. Miguel, L. Álvarez de Cienfuegos, J. Justicia, S. Abbate, E. Castiglioni, C. Bour, M. Ribagorda, D. J. Cárdenas, J. M. Paredes, L. Crovetto, D. Choquesillo-Lazarte, A. J. Mota, M. C. Carreño, G. Longhi and J. M. Cuerva, Stapled helical o-OPE foldamers as new circularly polarized luminescence emitters based on carbophilic interactions with Ag(i)-sensitivity, *Chem. Sci.*, 2016, **7**, 5663-5670.

26 Y. Imai, Y. Nakano, T. Kawai and J. Yuasa, A Smart Sensing Method for Object Identification Using Circularly Polarized Luminescence from Coordination-Driven Self-Assembly, *Angew. Chem. Int. Ed.*, 2018, **57**, 8973-8978.

27 P. Reiné, J. Justicia, S. P. Morcillo, S. Abbate, B. Vaz, M. Ribagorda, Á. Orte, L. Álvarez de Cienfuegos, G. Longhi, A. G. Campaña, D. Miguel and J. M. Cuerva, Pyrene-Containing ortho-Oligo(phenylene)ethynylene Foldamer as a Ratiometric Probe Based on Circularly Polarized Luminescence, *J. Org. Chem.*, 2018, **83**, 4455-4463.

28 R. Yonenuma and H. Mori, Synthesis and self-assembly of a diphenylalanine–tetraphenylethylene hybrid monomer and RAFT polymers with aggregation-induced emission, *Polym. Chem.*, 2023, **14**, 1469-1477.

29 R. Yonenuma and H. Mori, RAFT-synthesis and self-assembly-induced emission of pendant diphenylalanine–tetraphenylethylene copolymers, *Soft Matter*, 2023, **19**, 8403-8412.

30 L. Pastor-Pérez, Y. Chen, Z. Shen, A. Lahoz and S.-E. Stiriba, Unprecedented Blue Intrinsic Photoluminescence from Hyperbranched and Linear Polyethylenimines: Polymer Architectures and pH-Effects, *Macromol. Rapid Commun.*, 2007, **28**, 1404-1409.

31 H. Lu, L. Feng, S. Li, J. Zhang, H. Lu and S. Feng, Unexpected Strong Blue Photoluminescence Produced from the Aggregation of Unconventional Chromophores in Novel Siloxane–Poly(amidoamine) Dendrimers, *Macromolecules*, 2015, **48**, 476-482.

32 R.-b. Wang, W.-z. Yuan and X.-y. Zhu, Aggregation-induced emission of non-conjugated poly(amido amine)s: Discovering, luminescent mechanism understanding and bioapplication, *Chin. J. Polym. Sci.*, 2015, **33**, 680-687.

33 R. Zhao, J. Zheng, Z. Chen, M. Wang, D. Zhang, L. Ding, C. Fu, C. Zhang and K. Deng, Synthesis and Aggregation-Induced Emission of Polyamide-Amines as Fluorescent Switch Controlled by Hg2+-Glutathione, *ChemistrySelect*, 2022, **7**, e202103562.

34 B. Saha, B. Ruidas, S. Mete, C. D. Mukhopadhyay, K. Bauri and P. De, AIE-active non-conjugated poly(N-vinylcaprolactam) as a fluorescent thermometer for intracellular temperature imaging, *Chem. Sci.*, 2020, **11**, 141-147.

35 S. Prasad, I. Mandal, S. Singh, A. Paul, B. Mandal, R. Venkatramani and R. Swaminathan, Near UV-Visible electronic absorption originating from charged amino acids in a monomeric protein, *Chem. Sci.*, 2017, **8**, 5416-5433.

36 X. Chen, W. Luo, H. Ma, Q. Peng, W. Z. Yuan and Y. Zhang, Prevalent intrinsic emission from nonaromatic amino acids and poly(amino acids), *Sci. China: Chem.*, 2018, **61**, 351-359.

37 R. Ravanfar, C. J. Bayles and A. Abbaspourrad, Structural Chemistry Enables Fluorescence of Amino Acids in the Crystalline Solid State, *Cryst. Growth Des.*, 2020, **20**, 1673-1680.

38 H. Zhang, Z. Zhao, P. R. McGonigal, R. Ye, S. Liu, J. W. Y. Lam, R. T. K. Kwok, W. Z. Yuan, J. Xie, A. L. Rogach and B. Z. Tang, Clusterization-triggered emission: Uncommon luminescence from common materials, *Materials Today* 2020, **32**, 275-292.

39 W. Zhang Yuan and Y. Zhang, Nonconventional macromolecular luminogens with aggregation-induced emission characteristics, *J. Polym. Sci., Part A: Polym. Chem.*, 2016, **55**, 560-574.

40 K. Bauri, B. Saha, A. Banerjee and P. De, Recent advances in the development and applications of nonconventional luminescent polymers, *Polym. Chem.*, 2020, **11**, 7293-7315.

41 H. Zhang and B. Z. Tang, Through-Space Interactions in Clusteroluminescence, *JACS Au*, 2021, **1**, 1805-1814.

42 X. Dou, Q. Zhou, X. Chen, Y. Tan, X. He, P. Lu, K. Sui, B. Z. Tang, Y. Zhang and W. Z. Yuan, Clustering-Triggered Emission and Persistent Room Temperature Phosphorescence of Sodium Alginate, *Biomacromolecules*, 2018, **19**, 2014-2022.

43 L.-L. Du, B.-L. Jiang, X.-H. Chen, Y.-Z. Wang, L.-M. Zou, Y.-L. Liu, Y.-Y. Gong, C. Wei and W.-Z. Yuan, Clustering-triggered Emission of Cellulose and Its Derivatives, *Chin. J. Polym. Sci.*, 2019, **37**, 409-415.

44 Q. Zhou, B. Cao, C. Zhu, S. Xu, Y. Gong, W. Z. Yuan and Y. Zhang, Clustering-Triggered Emission of Nonconjugated Polyacrylonitrile, *Small*, 2016, **12**, 6586-6592.

45 Q. Zhou, Z. Wang, X. Dou, Y. Wang, S. Liu, Y. Zhang and W. Z. Yuan, Emission mechanism understanding and tunable persistent room temperature phosphorescence of amorphous nonaromatic polymers, *Mater. Chem. Front.*, 2019, **3**, 257-264.

46 Q. Huang, J. Cheng, Y. Tang, Y. Wu, D. Xia, Y. Zheng and M. Guo, Significantly Red-Shifted Emissions of

Nonconventional AIE Polymers Containing Zwitterionic Components, *Macromol. Rapid Commun.*, 2021, **42**, e2100174.

47 Y. Du, X. Xue, Q. Jiang, W. Huang, H. Yang, L. Jiang, B. Jiang and S. Komarneni, Tunable Multicolor Luminescence Polyglycidol-Acrylates: One-Pot Preparation and Properties, *ACS Appl. Polym. Mater.*, 2023, **5**, 3817-3826.

48 P. Liao, S. Zang, T. Wu, H. Jin, W. Wang, J. Huang, B. Z. Tang and Y. Yan, Generating circularly polarized luminescence from clusterization‐triggered emission using solid phase molecular self-assembly, *Nat. Commun.*, 2021, **12**, 5496.

49 M. Zhou, Y. Gong, Y. Yuan and H. Zhang, Research on Circularly Polarized Luminescent and Clustering-Triggered Emission Properties of Cholesteryl Benzoate, *J. Phys. Chem. C*, 2022, **126**, 15485-15490.

50 Y. Liu, S. Yang, B. Zhao and J. Deng, Nonconventional Fluorescence-Based Circularly Polarized Luminescent Core/Shell Particles: Maleic Anhydride Copolymer as the Core and Chiral Helical Polyacetylene as the Shell, *ACS Macro Lett.*, 2023, **12**, 530-535.

51 M. Zhou, J. Zhang, Y. Chen, Z. Chen, Y. Yuan, Y. Gong and H. Zhang, Clustering-Triggered Emission Liquid Crystalline Polymer Bearing Cholesterol: Tunable Circularly Polarized Luminescence and Room-Temperature Phosphorescence, *Macromol. Rapid Commun.*, 2023, **44**, 2300449.

52 T. Koseki, R. Kanto, R. Yonenuma, K. Nakabayashi, H. Furusawa, S. Yano and H. Mori, Multi-stimuli-responsive chiral-achiral ampholytic block copolymers composed of poly(N-acryloyl amino acid) and poly(vinyl amine), *React. Funct. Polym.*, 2020, **150**, 104540.

53 R. Kanto, R. Yonenuma, M. Yamamoto, H. Furusawa, S. Yano, M. Haruki and H. Mori, Mixed Polyplex Micelles with Thermoresponsive and Lysine-Based Zwitterionic Shells Derived from Two Poly(vinyl amine)-Based Block Copolymers, *Langmuir*, 2021, **37**, 3001-3014.

54 Y. Tani, R. Yonenuma and H. Mori, Clusterization-triggered emission of poly(vinyl amine)-based ampholytic block and random copolymers, *React. Funct. Polym.*, 2023, **184**, 105518.

55 Y. Tani, R. Yonenuma, S. Yano, H. Furusawa and H. Mori, Clusterization-triggered emission, stimulus-responsiveness, and DNA polyplex formation of poly(vinylamine)-based chiral block and random copolymers, *Eur. Polym. J.*, 2024, **208**, 112889.

56 Y. Maki, H. Mori and T. Endo, Controlled RAFT Polymerization of N-Vinylphthalimide and its Hydrazinolysis to Poly(vinyl amine), *Macromol. Chem. Phys.*, 2007, **208**, 2589-2599.

57 Y. Maki, H. Mori and T. Endo, Synthesis of Amphiphilic and Double-Hydrophilic Block Copolymers Containing Poly(vinyl amine) Segments by RAFT Polymerization of N-Vinylphthalimide, *Macromol. Chem. Phys.*, 2010, **211**, 45-56.

58 L. Bai, H. Yan, T. Bai, Y. Feng, Y. Zhao, Y. Ji, W. Feng, T. Lu and Y. Nie, High Fluorescent Hyperbranched Polysiloxane Containing β-Cyclodextrin for Cell Imaging and Drug Delivery, *Biomacromolecules*, 2019, **20**, 4230-4240.

59 C. Diaferia, V. Roviello, G. Morelli and A. Accardo, Self-Assembly of PEGylated Diphenylalanines into Photoluminescent Fibrillary Aggregates, *ChemPhysChem*, 2019, **20**, 2774-2782.

60 D. Urry and J. Krivacic, Differential scatter of left and right circularly polarized light by optically active particulate systems, *Proceedings of The National Academy of Science*, 1970, **65**, 845-852.

61 D. J. Gordon and G. Holzwarth, Optical activity of membrane suspensions. Calculation of artifacts by Mie scattering theory *Proceedings of The National Academy of Science of The United States of America*, 1971, **68**, 2365-2369.

62 D. J. Gordon, Classical scattering calculation of particulate artifacts in membrane optical activity, *ANNALS of The New York Academy of Sciences*, 1972, **195**, 147-149.

63 D. J. Gordon, Mie scattering by optically active particles, *Biochemistry* 1972, **1974**, 413-420.

64 G. Holzwarth, D. G. Gordon, J. E. McGinness, B. P. Dorman and M. F. Maestre, ie scattering contributions to the optical density and circular dichroism of T2 bacteriophage, *Biochemistry*, 1974, **13**, 126-132.

65 H. Zhang, H. Wei, L. Xu, Y. Li, Z. Song, D. Zhou, Q. Wang, Z. Long, Y. Yang, Y. Wen, G. Han, Y. Gao and J. Qiu, Chiral inorganic nanostructured BiOCl co-doped with Er^{3+}/Yb^{3+} exhibits circularly polarized luminescence and enhanced upconversion luminescence, *Ceramics International*, 2023, **49** 30436-30442.

66 R. Yonenuma, A. Ishizuki, K. Nakabayashi and H. Mori, Synthesis and Hierarchical Self‐Assembly of Diphenylalanine‐Based Homopolymer and Copolymers By RAFT Polymerization, *J. Polym. Sci., Part A: Polym. Chem.*, 2019, **57**, 2562-2574.

67 Y. Ma, H. Zhang, K. Wang, D. Cao, K. Wang, R. Guan and C. Zhou, The bright fluorescence of non-aromatic molecules in aqueous solution originates from pH-induced CTE behavior, *Spectrochim. Acta A Mol. Biomol. Spectrosc.*, 2021, **254**, 119604.

68 M. B. Avinash and T. Govindaraju, A bio-inspired design strategy: Organization of tryptophan-appended naphthalenediimide into well-defined architectures induced by molecular interactions, *Nanoscale*, 2011, **3**, 2536-2543.

69 S. Sun, S. Xu, W. Zhang, P. Wu, W. Zhang and X. Zhu, Cooperative self-assembly and crystallization into fractal patterns by PNIPAM-based nonlinear multihydrophilic block copolymers under alkaline conditions, *Polym. Chem.*, 2013, **4**, 5800-5809.

70 Y.-J. Chao, K. Wu, H.-H. Chang, M.-J. Chien and J. C. C. Chan, Manifold of self-assembly of a de novo designed

peptide: amyloid fibrils, peptide bundles, and fractals, *RSC Adv.*, 2020, **10**, 29510-29515.

71 V. Castelletto and I. W. Hamley, Self assembly of a model amphiphilic phenylalanine peptide/polyethylene glycol block copolymer in aqueous solution, *Biophys. Chem.*, 2009, **141**, 169-174.

72 M. Biancalana and S. Koide, Molecular mechanism of Thioflavin-T binding to amyloid fibrils, *Biochim. Biophys. Acta Proteins Proteom.*, 2010, **1804**, 1405-1412.

73 N. U. Deshpande, M. Virmani and M. Jayakannan, An AIE-driven fluorescent polysaccharide polymersome as an enzyme-responsive FRET nanoprobe to study the real-time delivery aspects in live cells, *Polym. Chem.*, 2021, **12**, 1549-1561.

74 S. Nobe, K. Yamamoto, H. Miyakawa, S. Yano, H. Furusawa and H. Mori, Sulfonium-cation-containing aggregation-induced emission block copolymers: self-assembly, multicolor emission, and detection for DNA polyplexes, *Eur. Polym. J.*, 2023, **197**, 112359.

75 A. I. Sulatskaya, A. A. Maskevich, I. M. Kuznetsova, V. N. Uversky and K. K. Turoverov, Fluorescence Quantum Yield of Thioflavin T in Rigid Isotropic Solution and Incorporated into the Amyloid Fibrils, *PLoS ONE*, 2010, **5**, e15385.

76 A. I. Sulatskaya, I. M. Kuznetsova and K. K. Turoverov, Interaction of Thioflavin T with Amyloid Fibrils: Fluorescence Quantum Yield of Bound Dye, *J. Phys. Chem. B*, 2012, **116**, 2538-2544.

77 G. Gorbenko, V. Trusova, T. Deligeorgiev, N. Gadjev, C. Mizuguchi and H. Saito, Two-step FRET as a tool for probing the amyloid state of proteins, *Journal of Molecular Liquids*, 2019, **294**, 111675.

78 A. I. Sulatskaya, A. V. Lavysh, A. A. Maskevich, I. M. Kuznetsova and K. K. Turoverov, Thioflavin T fluoresces as excimer in highly concentrated aqueous solutions and as monomer being incorporated in amyloid fibrils, *Sci. Rep.*, 2017, **7**, 2146.

79 A. Rybicka, G. Longhi, E. Castiglioni, S. Abbate, W. Dzwolak, V. Babenko and M. Pecul, Thioflavin T: Electronic Circular Dichroism and Circularly Polarized Luminescence Induced by Amyloid Fibrils, *ChemPhysChem*, 2016, **17**, 2931-2937.

Data availability statement

The data supporting this article have been included as part of the Supplementary Information.